

Adrenomedullin Expression and Growth Inhibitory Effects in Distinct Pulmonary Artery Smooth Muscle Cell Subpopulations

Paul D. Upton, John Wharton, Hedley Coppock, Neil Davie, Xudong Yang, Magdi H. Yacoub, Mohammad A. Ghatei, Julia M. Polak, Stephen R. Bloom, David M. Smith, and Nicholas W. Morrell

Section on Clinical Pharmacology, Departments of Histochemistry, Metabolic Medicine, and Cardiothoracic Surgery, Imperial College School of Medicine, London, United Kingdom

The vasodilator peptide adrenomedullin is elevated in patients with pulmonary hypertension and has been implicated in the inhibition of vascular remodeling. We questioned whether adrenomedullin is released by human pulmonary artery smooth muscle cells (PASMCs) and inhibits PASMC growth and release of endothelin, a known smooth muscle cell mitogen. The majority of PASMCs isolated from proximal pulmonary arteries and all PASMCs from distal pulmonary arteries released adrenomedullin, although at differing rates (mean, 177 ± 28 and 62 ± 11 fmol/ 10^5 cells/24 h, respectively). These cells were designated ADM(+). However, some proximal PASMC isolates did not release adrenomedullin, designated ADM(-). Northern blot analysis confirmed adrenomedullin expression in proximal ADM(+) but not ADM(-) isolates. ADM(-) and distal ADM(+) PASMCs proliferated faster in serum than did proximal ADM(+) cells. Adrenomedullin potently and dose-dependently (mean $EC_{50} = 2.2 \pm 0.5$ nM) increased intracellular cyclic adenosine monophosphate (cAMP) in ADM(-) isolates via specific adrenomedullin receptors. In contrast, both adrenomedullin and calcitonin gene-related peptide modestly elevated cAMP in 50% of ADM(+) isolates. Adrenomedullin dose-dependently inhibited platelet-derived growth factor-stimulated [3 H]thymidine incorporation and endothelin release in ADM(-) cells but did not affect [3 H]thymidine uptake in ADM(+) isolates. We conclude that distinct subpopulations of human PASMCs release and respond to adrenomedullin. The heterogeneity of adrenomedullin release and the inhibition of PASMC DNA synthesis and endothelin release suggest that adrenomedullin may function as a paracrine mediator in the inhibition of pulmonary vascular remodeling.

Adrenomedullin is constitutively secreted by systemic vascular endothelial and smooth muscle cells (VSMCs) (1, 2) and is expressed at a high level in the lung (3, 4). Specific binding sites for adrenomedullin are widespread in rat tissues, with the highest density found in the lung (5). Adrenomedullin binding sites have also been demonstrated in rat aorta and VSMCs (6, 7). Adrenomedullin

can bind either to specific adrenomedullin receptors or, with less affinity, to calcitonin gene-related peptide (CGRP₁) receptors, whereas CGRP does not bind to adrenomedullin receptors (5, 8). Thus, the cardiovascular effects of adrenomedullin and CGRP may overlap considerably as a result of receptor promiscuity.

In vivo studies have demonstrated that adrenomedullin is a potent vasodilator in the systemic (6, 9) and pulmonary circulations (10, 11). However, adrenomedullin has also been implicated as a modulator of vascular remodeling because the peptide inhibits migration (12, 13) and proliferation of systemic VSMCs (14). These antitrophic effects of adrenomedullin are believed to be mediated, at least in part, by elevation of intracellular cyclic adenosine monophosphate (cAMP) (12, 14, 15). The antiproliferative and vasodilator effects of adrenomedullin may be enhanced by its ability to inhibit release of endothelin (ET)-1, a potent vasoconstrictor and VSMC mitogen, from rat endothelial cells, systemic VSMCs, and aortic rings (15–17).

Several lines of evidence suggest a role for adrenomedullin in modulating pulmonary vascular tone and cell growth during the development of pulmonary hypertension. Plasma adrenomedullin levels are raised in patients with either primary or secondary pulmonary hypertension (18) and in rats with monocrotaline-induced hypertension (19). In addition, binding sites for adrenomedullin are increased in the lungs of rats with hypoxia-induced hypertension (11). Furthermore, a recent study showed that chronic infusion of adrenomedullin markedly reduced the pulmonary hypertension and pulmonary arterial medial thickening in monocrotaline-treated rats (20). Therefore, we hypothesized that adrenomedullin might be an important inhibitor of the VSMC proliferation and hypertrophy observed in pulmonary vascular remodeling (21). Our approach involved characterization of adrenomedullin release and adrenomedullin receptor mediated cAMP elevation in primary cultures of smooth muscle cells derived from the human pulmonary artery. In addition, we investigated the potential of adrenomedullin to inhibit the growth of human pulmonary artery smooth muscle cells (PASMCs) and its effect on release of endothelin, a mitogen widely implicated in the pathogenesis of pulmonary hypertension (22, 23).

Materials and Methods

Reagents

Medium 199 (M199), type II collagenase, fetal bovine serum (FBS), antibiotic/antimycotic solution, and trypsin-ethylenediaminetetraacetic acid (EDTA) were purchased from Life Technologies (Paisley, Renfrewshire, UK). Accutase, smooth muscle cell me-

(Received in original form April 10, 2000 and in revised form August 11, 2000)

Address correspondence to: Nicholas W. Morrell, M.D., Dept. of Medicine, Box 157, Level 5, Addenbrookes Hospital, Cambridge, UK CB2 2QQ.

Abbreviations: analysis of variance, ANOVA; bovine serum albumin, BSA; cyclic adenosine monophosphate, cAMP; calcitonin gene-related peptide, CGRP; dibutyl cAMP, dbcAMP; ethylenediaminetetraacetic acid, EDTA; endothelin, ET; fetal bovine serum, FBS; fast protein liquid chromatography, FPLC; 3-isobutyl-1-methylxanthine, IBMX; immunoglobulin, Ig; dissociation constant, K_d ; medium 199, M199; pulmonary artery smooth muscle cell, PASMC; phosphate-buffered saline, PBS; platelet-derived growth factor, PDGF; radioimmunoassay, RIA; sodium dodecyl sulfate, SDS; standard error of the mean, SEM; serum-free medium, SFM; saline sodium citrate, SSC; vascular smooth muscle cell, VSMC.

dium (SMCM), and growth supplement (GS) (containing insulin, human epidermal growth factor, human fibroblast growth factor and 5% FBS) were purchased from TCS Biologicals Ltd. (Botolph Claydon, Buckinghamshire, UK). Human adrenomedullin(1-52) and human adrenomedullin(22-52) were synthesized by Dr. P. Byfield (Clinical Science Centre, Hammersmith Hospital, London, UK). Rat adrenomedullin was purchased from Peptide Institute (Osaka, Japan). Na¹²⁵I, [α -³²P]deoxycytidine triphosphate (dCTP), and MegaprimeTM DNA labeling system were purchased from Amersham Pharmacia Biotech (Little Chalfont, Bucks, UK). 5-chloromethylfluorescein diacetate was from Molecular Probes (Leiden, The Netherlands). Methyl-[³H]thymidine (6.7 Ci/mmol) was from ICN Biomedicals Ltd. (Thame, Oxfordshire, UK). Monoclonal antibodies to alpha-smooth muscle actin (IA4), human fibroblast surface protein (clone IB10), vimentin (clone V9), and fluorescein isothiocyanate (FITC)-conjugated antimouse immunoglobulin (Ig) G were purchased from Sigma (Poole, Dorset, UK). The antibodies to human proline-4-hydroxylase (clone 5B5) and CD31 (JC70A) were from Dako Ltd. (Ely, Cambridge, UK). CyTM3-conjugated anti-rabbit IgG was from Jackson ImmunoResearch Laboratories Inc. (West Grove, PA). Recombinant human platelet-derived growth factor (PDGF)-BB was from Sigma and all other reagents were from Sigma or Merck (Lutterworth, Leicestershire, UK).

Isolation of PASMCS

Proximal segments of human pulmonary artery (pulmonary trunk or right/left lobar pulmonary artery) were obtained from resected lung specimens from patients undergoing lung or heart-lung transplantation (four men, four women; mean age, 42.5 yr) for congenital heart disease ($n = 3$), emphysema ($n = 4$), or cystic fibrosis ($n = 1$). Further specimens were available from donor tissues at transplantation ($n = 5$) (four men, one woman; mean age, 35.3 yr). Ethical approval was obtained from the Hammersmith Hospital and Harefield Hospital Ethics Committees. PASMCS were isolated by collagenase digestion of the arterial media and maintained as previously described (24).

Distal PASMCS were isolated from peripheral regions of the lung obtained from resected lung specimens from patients (one man, four women; mean age, 54.6 yr) undergoing lung or heart-lung transplantation for primary pulmonary hypertension ($n = 2$) or emphysema ($n = 1$), or lobectomy for lung carcinoma ($n = 2$). Segments of artery (0.3 to 1.0 mm external diameter) and attached branches were carefully separated from the parenchyma and the adventitia was removed. Isolated arterial segments were then washed in phosphate-buffered saline (PBS), minced with a scalpel blade, and digested in type II collagenase (1,000 U/ml; Life Technologies) in serum-free M199 (SFM) at 37°C for 4 h. At 1-h intervals, the suspension was drawn through a 1-ml pipette five times and after 4 h, it was filtered (pore size, 100 μ m; Becton Dickinson, Franklin Lakes, NJ) and centrifuged at 200 $\times g$ for 5 min. Distal PASMCS were resuspended in SMCM-GS and plated in 6- to 12-well culture plates. The medium was changed every 2 d, and when cells were confluent, they were dissociated using accutase.

Serum-Induced Growth Response of PASMCS

Cells were seeded at a density of 1.5×10^4 cells/well in M199/10% FBS in 24-well plates. The day of plating was designated Day 0. Cells were replenished with fresh M199/10% FBS every 48 h. On the relevant days, four wells of each isolate were washed briefly with PBS, trypsinized with 0.25% trypsin-EDTA in PBS, and counted by hemocytometer. Viability was assessed by trypan blue exclusion.

Phenotypic Characterization of Cells

The smooth muscle phenotype of isolated cells was investigated with a monoclonal antismooth muscle alpha-actin antibody (IA4)

and a polyclonal antibody to smooth muscle-specific myosin (kindly provided by Dr. Maria Frid, University of Colorado Health Sciences Center, Denver, CO) (25). The possible presence of fibroblast and endothelial cell phenotypes was excluded using antibodies to human fibroblast surface protein, proline-4-hydroxylase, and CD31. Cells were seeded at a density of 5×10^3 cells/well in M199/10% FBS in 8-well slide chambers (Life Technologies) and grown for a further 2 d. Cells were fixed in methanol at -20°C for 10 min, then washed three times briefly in PBS at room temperature. Cells were incubated with primary antisera (1:100) for 1 h at room temperature and washed three times with PBS. FITC-conjugated antimouse IgG or CyTM3-conjugated anti-rabbit IgG secondary antibody was added as appropriate for 1 h at room temperature. Cells were counterstained with the nuclear stain 4,6-diamidino-2-phenylindole (0.5 μ g/ml in PBS) for 2 min, rinsed with PBS, and mounted in PBS:glycerol (1:1). Staining was visualized by fluorescence microscopy.

Determination of Cell Size by Fluorescence-Activated Cell Sorter

The relative cell size distribution of individual proximal PASMCS isolates was determined by flow cytometry using 5-chloromethylfluorescein diacetate (CMFDA) as a marker for intact cells (26). Confluent flasks of cells were trypsinized, and the cells were incubated with 0.4 μ g/ml CMTDA for 30 min in SFM. The cells were washed twice with PBS at 37°C. Single cell suspensions of equal density were resuspended in PBS and immediately measured for relative size distribution based on forward scatter (Coulter EPICS XL-MCL; Beckman Coulter Inc., High Wycombe, Buckinghamshire, UK). Forward scatter has been shown to correlate with cell size, and size was estimated from the forward scatter produced by 10- μ m beads (27).

Adrenomedullin Secretion Time Course

Cells were seeded at a density of 5×10^4 cells/well in 6-well plates and grown to 80 to 90% confluence. Cells were serum-starved by washing once with SFM and then incubating in SFM for 2 h. Serum-starved cells were incubated in 2 ml M199/0.1% FBS for 6, 10, 24, and 48 h. At the designated time point cells were counted and aliquots (1 ml) of culture medium were collected, frozen immediately, dried by rotary evaporation, and stored at -20°C . The dried samples were resuspended in assay buffer and submitted to radioimmunoassay (RIA) for adrenomedullin.

Adrenomedullin RIA

Samples were assayed for adrenomedullin immunoreactivity using a previously reported specific human RIA (28). Briefly, assays were performed in a final volume of 700 μ l assay buffer comprising 0.06 M sodium phosphate (pH 7.2) containing 0.3% (wt/vol) bovine serum albumin (BSA), 10 mM EDTA, and 7 mM sodium azide. The antibody (designated FB8) was used at a final dilution of 1:10,000. The tracer was prepared by iodination of synthetic human adrenomedullin(22-52) by the Iodogen method and purification of the [¹²⁵I]adrenomedullin(22-52) tracer by reversed-phase high performance liquid chromatography (HPLC) (8). Assays were incubated at 4°C for 3 d. Bound and free tracers were separated using dextran-coated charcoal. The detection limit of the assay was 2 fmol/tube and the intra- and interassay coefficients of variation were 2.8 and 11.1%, respectively.

Characterization of Adrenomedullin Immunoreactivity in PASMCS Conditioned Medium

Characterization of immunoreactive adrenomedullin detected in conditioned medium was performed using fast protein liquid chromatography (FPLC) (Pharmacia, St. Albans, Hertfordshire, UK). For conditioning of medium, cells were grown to 80 to 90% con-

fluence in T75 flasks. The cells were serum-starved for 2 h followed by incubation in 12 ml of M199/0.1% FBS for 24 h. The conditioned medium was acidified with glacial acetic acid to a concentration of 0.5 M and extracted using Sep-Pak C₁₈ cartridges (Waters, Watford, Hertfordshire, UK) as previously described (29).

FPLC of extracted medium was performed according to a previously published protocol (8). Dried samples were resuspended in water containing 0.1% trifluoroacetic acid, loaded onto a PepRPC C₂/C₁₈ reversed-phase column, and eluted with a linear gradient of 10 to 50% acetonitrile over 60 min. Fractions collected over 1-min periods were dried by rotary evaporation and submitted to RIA for adrenomedullin.

Northern Blot Analysis of Adrenomedullin Messenger RNA

To extract total RNA, 10⁶ to 10⁷ cells were trypsinized followed by centrifugation at 200 × *g* for 5 min. The cell pellets were lysed in Trizol reagent (Life Technologies), and total RNA was extracted according to the manufacturer's instructions. Total RNA (50 μg) was fractionated using denaturing 3-(*N*-morpholino)propane-sulfonic acid/formaldehyde/1% agarose gels, and transferred to Hybond-N nylon membranes (Amersham Pharmacia Biotech), followed by ultraviolet cross-linking.

Membranes were hybridized with a 900-bp complementary DNA (cDNA) probe, which includes the coding sequence for human adrenomedullin (3). The probe was labeled by the random primer method using the Megaprime™ DNA labeling kit (Amersham Pharmacia Biotech). Briefly 10 ng of the cDNA probe was mixed with the primers, boiled for 5 min, and cooled on ice. The reaction buffer containing deoxyadenosine triphosphate, deoxythymidine triphosphate, and deoxyguanosine triphosphate was added together with [α-³²P]dCTP and the Klenow fragment of DNA polymerase. The reaction was incubated at 37°C for 1 h and terminated by addition of three volumes of Tris/EDTA/SDS (TES) buffer (10 mM Tris HCl, pH 7.5, containing 1 mM EDTA, pH 8.0, and 0.1% [wt/vol] sodium dodecyl sulfate [SDS]). The membranes were prehybridized in 30 ml of 5× saline sodium citrate (SSC) (1× = 0.15 M NaCl, 0.015 M sodium citrate, pH 7.0), 5× Denhardt's (1× = 0.025% polyvinylpyrrolidone, 0.02% Ficoll, 0.02% BSA), 1% SDS, and 5 ng/ml salmon sperm DNA (Life Technologies) for 2 h at 60°C. Hybridization was performed overnight at 60°C in 15 ml of prehybridization buffer plus 10% (wt/vol) dextran sulfate. Membranes were washed once with 2× SSC/0.2% SDS at 22°C for 10 min followed by 0.2× SSC/0.1% SDS at 60°C for 60 min. Washed membranes were exposed to Kodak Biomax MR-1 film (Sigma) at -70°C for 1 to 3 d. Membranes were then stripped of radioactive probe by incubation in 1× Tris/EDTA (TE) (10 mM Tris HCl, pH 7.5, containing 1 mM EDTA, pH 8.0) containing 0.5% (wt/vol) SDS for 15 min at 80°C. The stripped membrane was then checked for RNA loading using an adaptation of the method described by Herrin and Schmidt (30). Briefly, the membrane was soaked in 5% acetic acid at 22°C for 15 min and then immersed in 0.5 M sodium acetate (pH 5.2) containing 0.04% (wt/vol) methylene blue for 10 min. The membrane was then destained by washing in 20% ethanol until the 28S and 18S ribosomal RNA bands were clearly visible.

Effect of Adrenomedullin on Intracellular cAMP Accumulation

To determine whether isolates possessed functional adrenomedullin or CGRP receptors, the effect of these peptides upon intracellular cAMP accumulation was measured. PASMCS were seeded at a density of 1.5 × 10⁴ cells/well in 24-well plates and grown to confluence. On the day of the experiment, cells were serum-starved for 3 h, then treated with peptides in SFM containing 50 μM 3-isobutyl-1-methylxanthine (IBMX) for 15 min as previously described (29). After treatment, cells were extracted overnight at

-20°C in 250 μl acid ethanol (75% ethanol, 16 mM HCl). Extracts were dried and assayed for cAMP content using a commercially available RIA kit (DuPont, Stevenage, Hertfordshire, UK).

Ligand Binding Studies in Cultured Cells

Ligand binding studies in cultured cells were performed as previously described (29). Briefly, PASMCS were seeded at a density of 1.5 × 10⁴ cells/well in 24-well plates precoated with poly-L-lysine and grown to confluence. For adrenomedullin binding, cells were incubated for 60 min at 4°C in 0.5 ml binding buffer (20 mM *N*-2-hydroxyethylpiperazine-*N'*-ethane sulfonic acid, pH 7.4, 5 mM MgCl₂, 10 mM NaCl, 4 mM KCl, 1 mM EDTA, 1 μM phosphoramidon, and 0.3% BSA) containing 1,000 becquerels (Bq) (200 pM) ¹²⁵I-rat adrenomedullin. Nonspecific binding was determined in the presence of excess (500 nM) unlabeled rat adrenomedullin. For equilibrium competition experiments, the concentration of unlabeled adrenomedullin was varied from 0 to 500 nM. For CGRP binding, cells were incubated for 45 min at 22°C in 0.5 ml adrenomedullin binding buffer containing 0.1% (wt/vol) BSA and 1,000 Bq (56 pM) ¹²⁵I-[Tyr⁰]αCGRP (8). Nonspecific binding was determined in the presence of excess (1 μM) unlabeled αCGRP.

After incubation, cells were washed twice with 0.5 ml ice-cold assay buffer and lysed with 1 M NaOH for counting bound ¹²⁵I peptide. Binding data were analyzed by nonlinear regression using Receptor-Fit (Lundon Software, Cleveland, OH) to calculate the dissociation constant (*K*_d).

Effect of Adrenomedullin on PDGF-BB-Stimulated Mitogenesis

The effect of adrenomedullin on basal or PDGF-stimulated mitogenesis in human PASMCS was determined by measurement of [³H]thymidine incorporation as previously described (24). Briefly, cells were seeded in 24-well plates at a density of 1.5 × 10⁴ cells/well, grown to 80 to 90% confluence, and then quiesced by serum starvation for 2 h followed by exposure to M199/0.1% FBS for 72 h. To determine the effect of adrenomedullin on basal or PDGF-stimulated mitogenesis, quiescent cells were incubated in M199/0.1% FBS with or without 5 ng/ml PDGF-BB for 24 h in the presence or absence of 100 nM rat adrenomedullin. A role for cAMP in the observed responses was studied by the addition of adrenomedullin with or without 50 μM IBMX, a nonselective inhibitor of cAMP phosphodiesterases, or by addition of 0.1 mM dibutyryl cAMP (dbcAMP), a cell permeable cAMP analogue. To determine the dose-response to adrenomedullin, quiescent cells were incubated for 24 h in M199/0.1% FBS containing 50 μM IBMX and 5 ng/ml PDGF-BB alone or in the presence of human adrenomedullin (0.1 to 100 nM). All wells contained 0.5 μCi/well [methyl-³H]thymidine for the 24-h incubation period. The cells were washed and lysed, and the thymidine incorporation was determined by scintillation counting as previously described (24).

Effect of Adrenomedullin on Basal Endothelin Release

Cells were seeded in 24-well plates at a density of 1.5 × 10⁴ cells/well and grown to 80 to 90% confluence. Cells were quiesced as described previously followed by incubation for 24 h in M199/0.1% FBS alone or in the presence of rat adrenomedullin (0.1 to 100 nM). In additional wells, cells were treated with M199/0.1% FBS containing 0.1 mM dbcAMP. At the end of this period, the medium was removed and frozen immediately for subsequent endothelin RIA. The cells were trypsinized and counted by hemocytometer. Viability was assessed by trypan blue exclusion.

Samples were assayed for endothelin immunoreactivity using a previously reported specific RIA (31). Briefly, assays were performed in a final volume of 700 μl assay buffer comprising 0.06 M sodium phosphate (pH 7.2) containing 0.3% (wt/vol) BSA, 10 mM EDTA, and 7 mM sodium azide. The antibody (designated

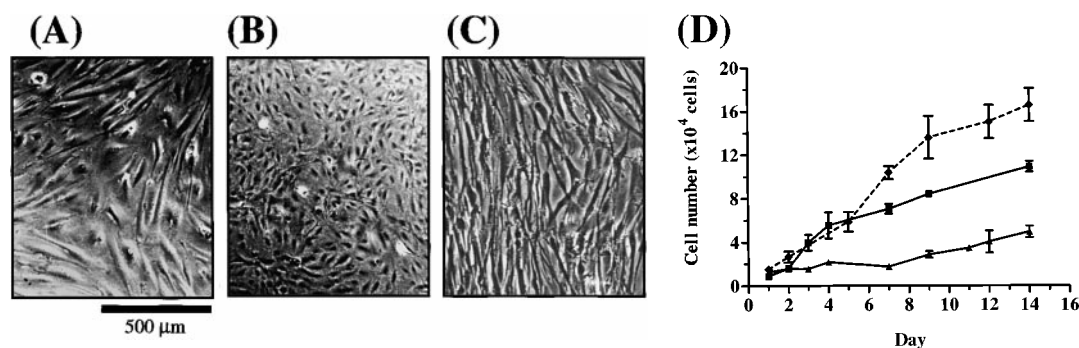


Figure 1. Phenotypic and growth characteristics of two distinct human proximal PASC isolates and distal PASC isolates designated ADM(+) or ADM(-) based on secretion or lack of secretion of adrenomedullin, respectively. Representative photomicrographs of the larger proximal ADM(+) PASCs (A), the smaller proximal

ADM(-) PASCs (B), and distal ADM(+) PASCs (C). The graph (D) shows the proliferation of human PASCs seeded at a density of 1.5×10^4 cells/well, grown in M199/10% FBS, and counted by hemocytometer on the days indicated. Points represent proximal ADM(+) (solid triangles, solid line), proximal ADM(-) (solid squares, solid line), and distal ADM(+) PASCs (solid diamonds, dashed line). Data are expressed as mean \pm SEM for four wells and are representative of at least two experiments for each isolate.

BP6) was used at a final dilution of 1:5,000. The [125 I]ET-1 tracer was prepared by iodination of synthetic human ET-1 using the Iodogen method and purified by reversed-phase HPLC. Assays were incubated at 4°C for 3 d. Bound and free tracers were separated using dextran-coated charcoal. The detection limit of the assay was 0.05 fmol/tube and the intra- and interassay coefficients of variation were 3.5 and 10.3%, respectively. This assay cross-reacts fully with ET-1 and displays 60% cross-reactivity and 40% cross-reactivity with ET-2 and ET-3, respectively.

Statistical Analyses

All data for response studies were analyzed by one-way analysis of variance (ANOVA) with *post hoc* Tukey's test using GraphPad Prism version 2.01 (GraphPad Software Inc., San Diego, CA). A paired Student's *t* test was used to compare cAMP responses to different agonists within an isolate.

Results

PASC Morphology and Growth Characteristics

Thirteen isolates from proximal pulmonary arteries were studied, each derived from a different subject. Five isolates from distal pulmonary arteries were studied, one of which was from the same subject as one of the proximal PASC isolates. The smooth muscle phenotype of all primary cultures was confirmed by the lack of immunoreactive human fibroblast surface protein, human proline-4-hydroxylase, and CD31, and positive immunofluorescent staining for vimentin, alpha smooth muscle actin, and smooth muscle-specific myosin. When viewed by conven-

tional phase contrast microscopy, individual proximal PASC isolates appeared to possess one of two distinct morphologies on the basis of cell size, nine isolates comprising large spindle-shaped cells (Figure 1A) and four isolates comprising small stellate cells (Figure 1B). In contrast, the distal PASCs (Figure 1C) displayed a similar morphology to the larger spindle-shaped proximal PASCs. This morphology is characteristic of PASCs we have isolated from main pulmonary arteries of 40 different patients (data not shown), whereas the small stellate cells have been isolated on only five occasions. There was no apparent association between the cellular phenotype of proximal PASCs and the disease or normal status of the patients. The phenotypic differences between the three cell types studied are summarized in Table 1. The apparent size difference between the proximal cell types was confirmed by differences in relative cell size on fluorescence-activated cell sorter analysis of cell suspensions (not shown). The stellate proximal PASCs had an estimated mean diameter of $32.5 \pm 9.5 \mu\text{m}$, whereas the spindle-shaped cells were $49.67 \pm 11.44 \mu\text{m}$. The stellate proximal cells and the distal PASCs demonstrated higher serum-stimulated growth rates than did the proximal spindle-shaped PASCs (Figure 1D).

Release of Immunoreactive Adrenomedullin from PASC

The larger spindle-shaped proximal PASC isolates ($n = 9$) and the distal PASC isolates ($n = 5$) secreted immu-

TABLE 1
PASC phenotypes, peptide release, and responses to adrenomedullin

	Proximal ADM(-)	Proximal ADM(+)	Distal ADM(+)
Growth in serum	+++	+	++
Size	Small	Large	Large
Morphology	Stellate	Spindle	Spindle
ADM release	-	+++	++
Endothelin release	+++	+	+
cAMP response to adrenomedullin	+++	+/-	+/-
ADM binding	++	-	-
Inhibition of [3 H]thymidine uptake by adrenomedullin	+++	-	-
Inhibition of endothelin release by adrenomedullin	+++	-	-

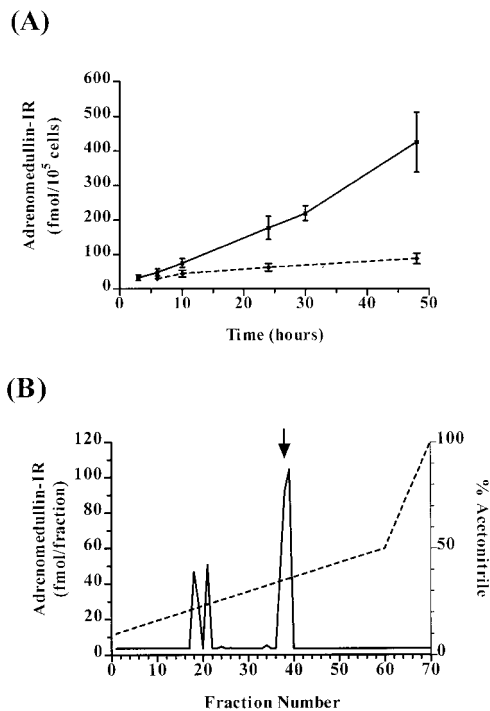


Figure 2. (A) Time course of adrenomedullin release from ADM(+) PASCs. Conditioned medium was removed at designated time points and stored until RIA for human adrenomedullin and cells counted by hemocytometer. Data are expressed as mean \pm SEM of the mean values for six proximal ADM(+) isolates (solid triangles, solid line) and four distal ADM(+) isolates (solid diamonds, dashed line). (B) FPLC of conditioned medium from ADM(+) PASCs eluted with a linear gradient of 10 to 50% acetonitrile over 60 min (dashed line) using a Pep-RPC C₂/C₁₈ FPLC column. Fractions collected over 1-min periods were dried and submitted for adrenomedullin RIA. The arrow indicates the elution position of synthetic human adrenomedullin.

noreactive adrenomedullin into the culture medium at an approximately linear rate and were designated ADM(+) (Figure 2A). The mean rate of adrenomedullin secretion by the proximal ADM(+) PASCs was significantly greater ($P < 0.05$) than that of distal ADM(+) cells (177 ± 28 versus 62 ± 11 fmol/ 10^5 cells/24 h). No immunoreactive adrenomedullin could be detected in the medium from the proximal stellate isolates described previously ($n = 4$) for up to 48 h. These isolates were designated ADM(-).

Reversed-phase FPLC separation of conditioned medium from ADM(+) cells showed that the majority of the immunoreactivity co-eluted with synthetic human adrenomedullin (Figure 2B), indicating that these cells release authentic adrenomedullin.

Expression of Adrenomedullin Messenger RNA

Northern blot analysis of total RNA from each isolate probed for adrenomedullin messenger RNA (mRNA) demonstrated a band of the expected 1.6 kb (3) in six proximal PASC ADM(+) isolates (Figure 3), whereas no signal was visible in the four ADM(-) isolates, even when the blots were overexposed (not shown). Staining of the filter with methylene blue confirmed the loading of RNA in all ten lanes.

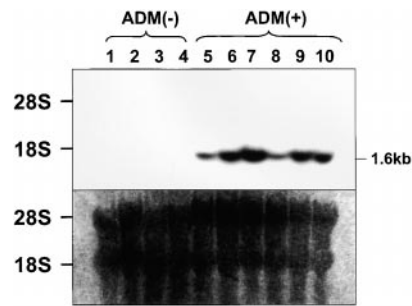


Figure 3. Northern blot of total RNA from proximal ADM(+) and ADM(-) cells probed with a ³²P-labeled adrenomedullin cDNA that included the full adrenomedullin coding region (upper panel). A 1.6-kb band is detected in ADM(+) cells as expected for human adrenomedullin. No hybridizing bands were observed on the lanes for the ADM(-) cells. Blots were stripped of radioactive probe and RNA loading checked by staining with methylene blue (lower panel).

Effect of Adrenomedullin on cAMP Accumulation

To determine whether PASCs possessed functional adrenomedullin receptors, the effect of adrenomedullin on intracellular cAMP accumulation was measured. Adrenomedullin dose-dependently increased intracellular cAMP in ADM(-) cells (Figure 4). The estimated mean EC₅₀ value for the increase in cAMP was 2.15 ± 0.55 nM. The mean basal cAMP concentration (4.5 ± 1.0 pmol/ 10^5 cells) increased to 104.4 ± 37.0 pmol/ 10^5 cells in the presence of 100 nM adrenomedullin. Human α CGRP (100 nM) also increased intracellular cAMP in ADM(-) cells (Figure 4) (mean 18.0 ± 7.6 pmol/ 10^5 cells), but the magnitude of the increase was only $16.6 \pm 2.8\%$ of the response to 100 nM adrenomedullin. The magnitude of the cAMP responses to adrenomedullin in the ADM(-) subpopulations differed markedly between isolates (Table 2).

In ADM(+) cells, two separate response profiles were evident. Two of five distal and five of nine proximal ADM(+) isolates demonstrated significant ($P < 0.05$) equipotent elevation of cAMP by either 100 nM adrenomedullin or 100 nM CGRP (Table 2, responsive ADM(+) PASCs), but the magnitude of this response was small compared with ADM(-) cells. In contrast, neither 100 nM adrenomedullin nor 100 nM CGRP stimulated intracellular cAMP in the remaining proximal or distal ADM(+) PASCs (Table 2, nonresponsive ADM(+) PASCs). The mean basal cAMP level in ADM(+) cells (3.9 ± 1.9

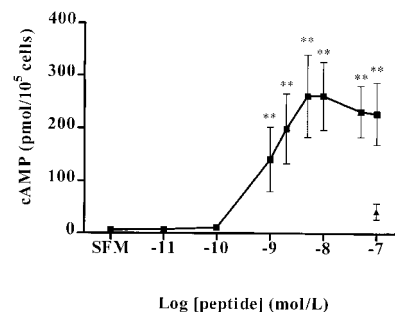


Figure 4. Stimulation of cAMP production by adrenomedullin in ADM(-) PASCs. Intracellular cAMP was measured ($n = 4$ wells per treatment) in the presence of 50 μ M IBMX with increasing concentrations of adrenomedullin (solid squares). Control or basal cAMP

was measured using SFM instead of adrenomedullin. CGRP (solid triangles) at 100 nM increased cAMP to a lesser extent that did adrenomedullin. Results are expressed as mean \pm SEM for three experiments with one representative isolate (PM1). $**P < 0.001$, one-way ANOVA with respect to SFM.

TABLE 2
Effects of adrenomedullin (100 nM) on cAMP, PDGF-stimulated thymidine uptake and endothelin release and CGRP (100 nM) on cAMP in ADM(+) isolates and individual ADM(-) isolates

Isolate Phenotype	cAMP (% of basal)		[³ H]Thymidine Inhibition by Adrenomedullin (% of PDGF)	ET-IR Release Inhibition by Adrenomedullin (% of control)
	Adrenomedullin	CGRP		
Nonresponsive ADM(+)	105 ± 4	107 ± 4	No effect	No effect
Responsive ADM(+)	148 ± 18*	146 ± 17*	No effect	No effect
ADM(-) PM4	820 ± 328*	183 ± 52	79.8 ± 6.4 [†]	87.3 ± 0.3 [‡]
ADM(-) PM3	1,818 ± 678 [†]	152 ± 29	86.4 ± 1.5 [†]	81.1 ± 9.2 [‡]
ADM(-) PM2	1,966 ± 479 [†]	417 ± 22 [†]	66.1 ± 2.0 [†]	66.9 ± 11.2 [‡]
ADM(-) PM1	3,780 ± 1,207 [‡]	667 ± 269 [†]	40.6 ± 4.3 [†]	38.6 ± 8.2 [‡]

**P* < 0.05 with respect to control for each experiment, one-way ANOVA with *post-hoc* Tukey's honest significant difference.

[†]*P* < 0.01 with respect to control for each experiment, one-way ANOVA with *post-hoc* Tukey's honest significant difference.

[‡]*P* < 0.001 with respect to control for each experiment, one-way ANOVA with *post-hoc* Tukey's honest significant difference.

pmol/10⁵ cells) was similar to that detected in ADM(-) cells (4.6 ± 1.0 pmol/10⁵ cells).

Binding Sites for Adrenomedullin and CGRP

To further characterize adrenomedullin binding sites on ADM(-) cells, radioligand binding studies were performed using ¹²⁵I-rat adrenomedullin, which is selective for adrenomedullin receptors (5). Specific binding of radiolabeled adrenomedullin demonstrated dose-dependent competition by unlabeled adrenomedullin in these cells. The highest specific binding in the ADM(-) isolates was observed in ADM(-) PM1 (Table 2) (mean specific binding, 31 ± 13 Bq/10⁵ cells; 17,811 ± 7,527 binding sites/cell) and was 51.5 ± 2.5% of total binding (*n* = 3 experiments). For this isolate, competition curves were constructed (Figure 5). The *K*_d for adrenomedullin was calculated to be 0.76 ± 0.16 nM (*n* = 3 experiments). Nonlinear regression analysis of the competition curves as one- or two-site fit models revealed adrenomedullin binding to be best explained by a single site. In contrast, a very low level of specific binding of [¹²⁵I]CGRP (mean specific binding, 4 ± 2 Bq/10⁵ cells) was observed in ADM(-) cells.

Growth Responses to Adrenomedullin

To determine whether adrenomedullin affected DNA synthesis in quiescent PSMCs, uptake of [methyl-³H]thymidine was studied in ADM(-) cells. Adrenomedullin (100 nM) had a small but significant (*P* < 0.05) inhibitory effect on basal 24-h [³H]thymidine uptake in two of the four

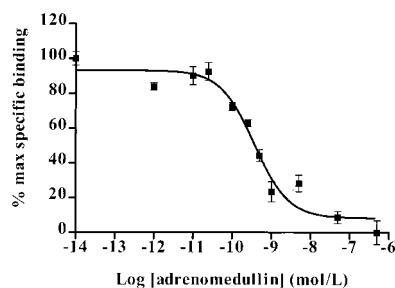


Figure 5. Equilibrium competition binding for [¹²⁵I]adrenomedullin with unlabeled adrenomedullin in ADM(-) PSMCs (PM1). The specific binding represented 51.5 ± 2.5% of the total binding. Data are expressed as a percentage of the maximum specific binding and are mean ± SEM for three wells. The graph is representative of three separate experiments.

isolates and are mean ± SEM for three wells. The graph is representative of three separate experiments.

ADM(-) isolates (data not shown). Incubation of ADM(-) cells with 100 nM adrenomedullin resulted in significant (*P* < 0.001) inhibition of PDGF-BB-stimulated [³H]thymidine uptake over 24 h in all four ADM(-) isolates (Figure 6A). This inhibitory effect of adrenomedullin was potentiated in the presence of 50 μM IBMX. The nonhydrolyzable cAMP analogue dbcAMP also significantly inhibited PDGF-BB-stimulated thymidine incorporation. The inhibitory effect of adrenomedullin, in the presence of 50 μM IBMX, was dose-dependent (Figure 6B). The magnitude of the inhibitory effect of adrenomedullin on PDGF-BB-stimulated thymidine uptake differed between the four ADM(-) isolates (Table 2).

In contrast, there was no effect of adrenomedullin on either basal or PDGF-BB-stimulated thymidine incorporation in any of the ADM(+) isolates, regardless of whether or not they demonstrated a cAMP response to adrenomedullin.

Effect of Adrenomedullin on Basal Immunoreactive Endothelin Release

ADM(-) cells released immunoreactive endothelin into the culture medium at a mean rate of 21.1 ± 4.0 fmol/10⁵ cells/24 h. In contrast, endothelin release from both distal and proximal ADM(+) cells was very low (highest rate, 0.2 fmol/10⁵ cells/24 h). Incubation of ADM(-) cells with adrenomedullin for 24 h resulted in a dose-dependent decrease in basal immunoreactive endothelin release (Figure 7). There were differences in the magnitude of basal ET-1 inhibition in the four ADM(-) isolates, with a tendency for a greater degree of inhibition in isolates with a greater increase in adrenomedullin-stimulated cAMP (Table 2). In addition, incubation of ADM(-) cells with 0.1 mM dbcAMP reduced endothelin release to a mean level of 15.2 ± 3.8% of basal endothelin release in ADM(-) isolates.

Discussion

The main finding of this study is that three subpopulations of smooth muscle cells derived from the human pulmonary arterial media are distinct with regard to expression of adrenomedullin and responsiveness to the growth inhibitory properties of this peptide. Isolates designated ADM(+) derived from either proximal or distal pulmo-

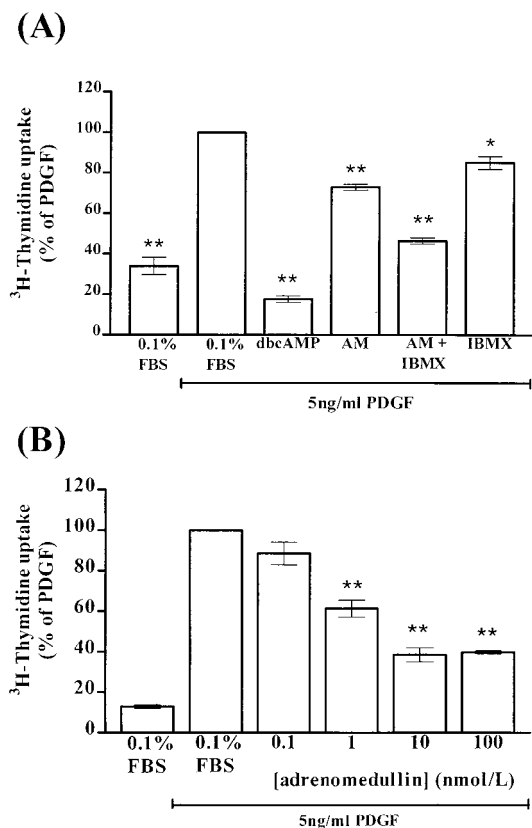


Figure 6. Inhibition of [³H]thymidine incorporation in ADM(−) PASMCs by adrenomedullin. (A) Cells were incubated with 5 ng/ml PDGF, and the effect of 100 nM adrenomedullin (AM) on [³H]thymidine uptake in the presence or absence of 50 μM IBMX was assessed. The effect of dbcAMP was also assessed. (B) Dose-dependent inhibitory effect of 0.1 to 100 nM adrenomedullin on PDGF-stimulated [³H]thymidine uptake. Data are representative of at least three experiments and are expressed as mean ± SEM. **P* < 0.01, ***P* < 0.001 with respect to PDGF.

nary arteries expressed and released adrenomedullin, but only released low levels of the potent vasoconstrictor and smooth muscle mitogen endothelin. These ADM(+) isolates were further distinguished as demonstrating either a modest cAMP elevation to adrenomedullin or CGRP, or no cAMP response to either peptide. In contrast, the second proximal PASMC phenotype, designated ADM(−), possessed functional adrenomedullin receptors and released high levels of endothelin but did not express adrenomedullin. Although distal and proximal ADM(+) PASMCs were similar in their morphology and size, the ADM(−) PASMCs were shown to be smaller by light microscopy and flow cytometry. However, the distal ADM(+) PASMCs and the ADM(−) PASMCs demonstrated substantially faster serum-stimulated growth rates compared with proximal ADM(+) isolates. Furthermore, we have identified a potential role for adrenomedullin in the paracrine inhibition of PASMC growth since adrenomedullin inhibited mitogen-stimulated DNA synthesis in ADM(−) cells via specific adrenomedullin receptors linked to elevation of intracellular cAMP. Adrenomedullin also inhibited release of endothelin by ADM(−) cells. These findings are

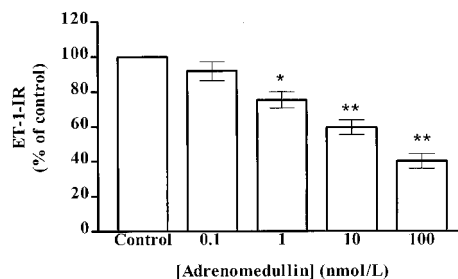


Figure 7. Adrenomedullin dose-dependently inhibits endothelin release from proximal ADM(−) PASMCs. Cells were treated with M199/0.1% FBS alone (Control) or with 0.1 to 100 nM adrenomedullin for 24 h. Data are the mean of at least three experiments and are expressed as mean ± SEM. **P* < 0.01, ***P* < 0.001 with respect to control.

consistent with the hypothesis that adrenomedullin may be an important paracrine inhibitor of pulmonary vascular remodeling. The main differences between the subpopulations of cells isolated in this study are summarized in Table 1.

We isolated thirteen vascular smooth muscle isolates from the tunica media of human proximal pulmonary arteries and five distal PASMC isolates. Immunostaining confirmed the smooth muscle cell phenotype of these isolates and eliminated the possibility of significant contamination by either fibroblasts or endothelial cells. Our findings suggest the presence of distinct subpopulations of cells within the proximal human pulmonary artery media and further differences between cells isolated from proximal and distal vessels. Heterogeneity of VSMCs in the bovine pulmonary arterial media is well recognized (25) with important functional implications for the regulation of vascular homeostasis. The morphologic characteristics of the smaller, fast-growing stellate cells identified in this study are similar to the faster growing cells identified in the adult bovine pulmonary artery media by Frid and coworkers (25). The larger, slower growing proximal PASMCs display morphologic characteristics similar to the more differentiated PASMCs found in the adult bovine pulmonary artery media (25). Our observations extend the concept of PASMC heterogeneity to humans and provide functional relevance for PASMC heterogeneity based on differential expression of adrenomedullin and receptors for adrenomedullin. Although not previously reported in isolated PASMCs, our finding of adrenomedullin expression and release is in accordance with previous reports showing high levels of adrenomedullin production by systemic VSMCs (2).

Adrenomedullin can bind to specific adrenomedullin receptors or CGRP₁ receptors on vascular cells (7, 32). A pulmonary vasodilator response to adrenomedullin has been demonstrated in animals (10, 33), and plasma adrenomedullin levels decrease across the human pulmonary circulation, implicating the pulmonary vasculature as an important site of clearance (34). Our data provide evidence for specific adrenomedullin receptors on human ADM(−) PASMCs. First, ADM(−) cells showed significant increases in intracellular cAMP with either adrenomedullin or CGRP, but the response to 100 nM adrenomedullin was consistently 6-fold greater than the response to an equiva-

lent dose of CGRP (29). Adrenomedullin increases intracellular cAMP in systemic vascular cells (13, 14, 32). Second, we demonstrated specific binding of [¹²⁵I]adrenomedullin, which is selective for adrenomedullin receptors (5, 32). The affinity of the binding sites ($K_d = 0.76 \pm 0.16$ nM) was similar to that previously reported for rat tissues (5, 6). In contrast to the large cAMP responses in ADM(-) PSMCs, small but significant cAMP elevations were elicited by 100 nM adrenomedullin or CGRP in half of the ADM(+) isolates, whereas the other half did not respond to either peptide. This small response to adrenomedullin or CGRP implies that receptors on the responsive ADM(+) isolates are downregulated or expressed at a low level. Reasons for this may include an artifact of the cells being in an *in vitro* environment, or as a result of receptor downregulation or fast turnover due to the high levels of adrenomedullin present in the culture medium. The observation that basal levels of cAMP were identical in ADM(+) and ADM(-) isolates implies that secreted adrenomedullin is not activating adrenomedullin receptors by autocrine feedback in ADM(+) cells. The low level of receptor expression in distal PSMCs is not inconsistent with the pulmonary vasorelaxation elicited by adrenomedullin *in vivo* because adrenomedullin may also indirectly mediate pulmonary vasodilation, stimulating nitric oxide release from endothelial cells (33).

Having established that ADM(-) cells possess functional receptors coupled to a adenylyl cyclase, we examined the effect of adrenomedullin on mitogenesis in these cells. Adrenomedullin caused a small reduction in basal thymidine incorporation in ADM(-) cells. Importantly, we did not observe stimulation of basal DNA synthesis by adrenomedullin in any of the isolates, as has been reported in quiescent rat VSMCs (35). Adrenomedullin significantly inhibited PDGF-BB-stimulated thymidine uptake in all four ADM(-) isolates, and the nonspecific phosphodiesterase inhibitor IBMX enhanced this response. The non-hydrolyzable cAMP analogue dbcAMP also significantly inhibited PDGF-stimulated mitogenesis. Adrenomedullin did not affect PDGF-BB-stimulated thymidine incorporation in any of the ADM(+) isolates, despite the low level increases in cAMP seen in these cells. The degree of inhibition of PDGF-stimulated mitogenesis by adrenomedullin seemed to reflect the relative levels of intracellular cAMP stimulated by adrenomedullin in proximal ADM(-) PSMCs, similar to a previous report in rat aortic VSMCs (14). Our results indicate that the inhibitory effect of adrenomedullin is likely to be mediated, at least in part, through adenylyl cyclase.

ET-1 is a potent vasoconstrictor peptide in human blood vessels and also stimulates mitogenesis in human PSMCs (22). In addition, plasma ET-1 is raised in patients with pulmonary hypertension (23). We demonstrated immunoreactive endothelin release by human PSMCs. Interestingly, ADM(+) and ADM(-) cells were distinct with regard to endothelin release, as ADM(-) cells secreted large amounts of endothelin into the medium, whereas the release from distal and proximal ADM(+) PSMCs was very low. Adrenomedullin has been reported to inhibit basal ET-1 release in systemic vascular cells (15, 16). In the present study, basal endothelin release from human

ADM(-) PSMCs was dose-dependently inhibited by adrenomedullin, and this effect was mimicked by dbcAMP. There was an apparent relationship between the stimulation of intracellular cAMP and inhibition of endothelin release by adrenomedullin in ADM(-) PSMCs. Interestingly, 0.1 mM dbcAMP inhibited mitogenesis and endothelin release to similar extents in ADM(-) PSMCs, whereas the magnitude of the responses to adrenomedullin differed considerably, probably reflecting differences in adrenomedullin receptor densities between isolates.

In conclusion, we have isolated two phenotypically distinct subpopulations of PSMCs from the proximal human pulmonary arterial media. These subpopulations differ with regard to cell size, serum-stimulated growth rates, adrenomedullin peptide and receptor expression, and release of endothelin. This apparent heterogeneity *in vitro* will require confirmation that these cell types coexist in the arterial wall. In addition, we also found differences between PSMCs isolated from proximal and distal vessels, in that the latter grew faster and released lower amounts of adrenomedullin. Furthermore, adrenomedullin inhibits PDGF-stimulated mitogenesis, probably via a cAMP-dependent mechanism. In addition, adrenomedullin inhibits ET-1 release in these cells. We demonstrated weak cAMP responses to adrenomedullin and CGRP in half of the proximal and distal ADM(+) isolates, implying these cells may also be responsive. We propose that adrenomedullin in the adult human pulmonary artery media acts as a paracrine inhibitor of smooth muscle cell growth, which may be partly mediated by attenuation of endothelin release.

Acknowledgments: The authors would like to thank Dr. Punit Ramrakha of the Division on Clinical Pharmacology, Hammersmith Hospital, for his assistance with flow cytometry. The human adrenomedullin probe was originally produced by Sanjeev Sharma, Department of Metabolic Medicine, Hammersmith Hospital.

This study was supported by grants PG/96121 and PG/99013 from the British Heart Foundation. N.M. is a Medical Research Council Clinician Scientist Fellow.

References

1. Sugo, S., N. Minamino, K. Kangawa, K. Miyamoto, K. Kitamura, J. Sakata, T. Eto, and H. Matsuo. 1994. Endothelial cells actively synthesize and secrete adrenomedullin. *Biochem. Biophys. Res. Commun.* 201:1160-1166. [Published erratum appears in *Biochem. Biophys. Res. Commun.* 203:1363.]
2. Sugo, S., N. Minamino, H. Shoji, K. Kangawa, K. Kitamura, T. Eto, and H. Matsuo. 1994. Production and secretion of adrenomedullin from vascular smooth muscle cells: augmented production by tumor necrosis factor- α . *Biochem. Biophys. Res. Commun.* 203:719-726.
3. Kitamura, K., J. Sakata, K. Kangawa, M. Kojima, H. Matsuo, and T. Eto. 1993. Cloning and characterization of cDNA encoding a precursor for human adrenomedullin. *Biochem. Biophys. Res. Commun.* 194:720-725. [Published erratum appears in *Biochem. Biophys. Res. Commun.* 202:643.]
4. Ichiki, Y., K. Kitamura, K. Kangawa, M. Kawamoto, H. Matsuo, and T. Eto. 1994. Distribution and characterization of immunoreactive adrenomedullin in human tissue and plasma. *FEBS Lett.* 338:6-10.
5. Owji, A. A., D. M. Smith, H. A. Coppock, D. G. Morgan, R. Bhogal, M. A. Ghatei, and S. R. Bloom. 1995. An abundant and specific binding site for the novel vasodilator adrenomedullin in the rat. *Endocrinology* 136:2127-2134.
6. Nandha, K. A., G. M. Taylor, D. M. Smith, A. A. Owji, P. G. Byfield, M. A. Ghatei, and S. R. Bloom. 1996. Specific adrenomedullin binding sites and hypotension in the rat systemic vascular bed. *Regul. Pept.* 62:145-151.
7. Eguchi, S., Y. Hirata, H. Kano, K. Sato, Y. Watanabe, T. X. Watanabe, K. Nakajima, S. Sakakibara, and F. Marumo. 1994. Specific receptors for adrenomedullin in cultured rat vascular smooth muscle cells. *FEBS Lett.* 340:226-230.
8. Owji, A. A., J. V. Gardiner, P. D. Upton, M. Mahmoodi, M. A. Ghatei, S. R. Bloom, and D. M. Smith. 1996. Characterisation and molecular identification of adrenomedullin binding sites in the rat spinal cord: a comparison

- with calcitonin gene-related peptide receptors. *J. Neurochem.* 67:2172–2179.
9. Ishiyama, Y., K. Kitamura, Y. Ichiki, S. Nakamura, O. Kida, K. Kangawa, and T. Eto. 1993. Hemodynamic effects of a novel hypotensive peptide, human adrenomedullin, in rats. *Eur. J. Pharmacol.* 241:271–273.
 10. Lippton, H., J. K. Chang, Q. Hao, W. Summer, and A. L. Hyman. 1994. Adrenomedullin dilates the pulmonary vascular bed in vivo. *J. Appl. Physiol.* 76:2154–2156.
 11. Zhao, L., L. A. Brown, A. A. Owji, D. J. Nunez, D. M. Smith, M. A. Gbatei, S. R. Bloom, and M. R. Wilkins. 1996. Adrenomedullin activity in chronically hypoxic rat lungs. *Am. J. Physiol.* 271:H622–H629.
 12. Horio, T., M. Kohno, H. Kano, M. Ikeda, K. Yasunari, K. Yokokawa, M. Minami, and T. Takeda. 1995. Adrenomedullin as a novel antimigration factor of vascular smooth muscle cells. *Circ. Res.* 77:660–664.
 13. Kohno, M., K. Yokokawa, H. Kano, K. Yasunari, M. Minami, T. Hanehira, and J. Yoshikawa. 1997. Adrenomedullin is a potent inhibitor of angiotensin II-induced migration of human coronary artery smooth muscle cells. *Hypertension* 29:1309–1313.
 14. Kano, H., M. Kohno, K. Yasunari, K. Yokokawa, T. Horio, M. Ikeda, M. Minami, T. Hanehira, T. Takeda, and J. Yoshikawa. 1996. Adrenomedullin as a novel antiproliferative factor of vascular smooth muscle cells. *J. Hypertens.* 14:209–213.
 15. Kohno, M., H. Kano, T. Horio, K. Yokokawa, K. Yasunari, and T. Takeda. 1995. Inhibition of endothelin production by adrenomedullin in vascular smooth muscle cells. *Hypertension* 25:1185–1190.
 16. Barker, S. and R. Corder. 1997. Adrenomedullin acts as a local mediator of vascular homeostasis through interactions which lead to reduced endothelin-1 synthesis and secretion. *J. Hum. Hypertens.* 11:605–606.
 17. Tian, Q., D. Zhao, D. Y. Tan, Y. T. Zhao, Q. H. Li, J. X. Qiu, L. W. Song, C. N. Gong, J. Yang, H. Lippton, et al. 1995. Vasodilator effect of human adrenomedullin(13-52) on hypertensive rats. *Can. J. Physiol. Pharmacol.* 73:1065–1069.
 18. Yoshibayashi, M., T. Kamiya, K. Kitamura, Y. Saito, K. Kangawa, T. Nishikimi, H. Matsuoka, T. Eto, and H. Matsuo. 1997. Plasma levels of adrenomedullin in primary and secondary pulmonary hypertension in patients < 20 years of age. *Am. J. Cardiol.* 79:1556–1558.
 19. Shimokubo, T., J. Sakata, K. Kitamura, K. Kangawa, H. Matsuo, and T. Eto. 1995. Augmented adrenomedullin concentrations in right ventricle and plasma of experimental pulmonary hypertension. *Life Sci.* 57:1771–1779.
 20. Yoshihara, F., T. Nishikimi, T. Horio, C. Yutani, S. Takishita, H. Matsuo, T. Ohe, and K. Kangawa. 1998. Chronic infusion of adrenomedullin reduces pulmonary hypertension and lessens right ventricular hypertrophy in rats administered monocrotaline. *Eur. J. Pharmacol.* 355:33–39.
 21. Hislop, A., and L. Reid. 1977. Changes in the pulmonary arteries of the rat during recovery from hypoxia-induced pulmonary hypertension. *Br. J. Exp. Pathol.* 58:653–662.
 22. Zamora, M. A., E. C. Dempsey, S. J. Walchak, and T. J. Stelzner. 1993. BQ123, an ETA receptor antagonist, inhibits endothelin-1-mediated proliferation of human pulmonary artery smooth muscle cells. *Am. J. Respir. Cell Mol. Biol.* 9:429–433.
 23. Stewart, D. J., R. D. Levy, P. Cernacek, and D. Langleben. 1991. Increased plasma endothelin-1 in pulmonary hypertension: marker or mediator of disease? *Ann. Intern. Med.* 114:464–469.
 24. Morrell, N. W., P. D. Upton, S. Kotecha, A. Huntley, M. H. Yacoub, J. M. Polak, and J. Wharton. 1999. Angiotensin II activates MAPK and stimulates growth of human pulmonary artery smooth muscle cells via AT₁ receptors. *Am. J. Physiol.* 277:L440–L448.
 25. Frid, M. G., E. P. Moiseeva, and K. R. Stenmark. 1994. Multiple phenotypically distinct smooth muscle cell populations exist in the adult and developing bovine pulmonary arterial media in vivo. *Circ. Res.* 75:669–681.
 26. Redelman, D., S. Butler, J. Robison, and D. Garner. 1988. Identification of inflammatory cells in bovine milk by flow cytometry. *Cytometry* 9:463–468.
 27. Jovin, T. M., S. J. Morris, G. Striker, H. A. Schultens, M. Digweed, and D. J. Arndt-Jovin. 1976. Automatic sizing and separation of particles by ratios of light scattering intensities. *J. Histochem. Cytochem.* 24:269–283.
 28. Meeran, K., D. O'Shea, P. D. Upton, C. J. Small, M. A. Gbatei, P. H. Byfield, and S. R. Bloom. 1997. Circulating adrenomedullin does not regulate systemic blood pressure but increases plasma prolactin after intravenous infusion in humans: a pharmacokinetic study. *J. Clin. Endocrinol. Metab.* 82:95–100.
 29. Coppock, H. A., A. A. Owji, C. Austin, P. D. Upton, M. L. Jackson, J. V. Gardiner, M. A. Gbatei, S. R. Bloom, and D. M. Smith. 1999. Rat-2 fibroblasts express specific adrenomedullin receptors, but not calcitonin-gene-related peptide receptors, which mediate increased intracellular cAMP and inhibit mitogen-activated protein kinase activity. *Biochem. J.* 338:15–22.
 30. Herrin, D. L., and G. W. Schmidt. 1988. Rapid, reversible staining of northern blots prior to hybridization. *Biotechniques* 6:196–200.
 31. Lam, H. C., K. Takahashi, M. A. Gbatei, and S. R. Bloom. 1990. Presence of immunoreactive endothelin in human milk. *FEBS Lett.* 261:184–186.
 32. Ishizaka, Y., M. Tanaka, K. Kitamura, K. Kangawa, N. Minamino, H. Matsuo, and T. Eto. 1994. Adrenomedullin stimulates cyclic AMP formation in rat vascular smooth muscle cells. *Biochem. Biophys. Res. Commun.* 200:642–646.
 33. Nossaman, B. D., C. J. Feng, A. D. Kaye, B. DeWitt, D. H. Coy, W. A. Murphy, and P. J. Kadowitz. 1996. Pulmonary vasodilator responses to adrenomedullin are reduced by NOS inhibitors in rats but not in cats. *Am. J. Physiol.* 270:L782–L789.
 34. Nishikimi, T., K. Kitamura, Y. Saito, K. Shimada, T. Ishimitsu, M. Takamiya, K. Kangawa, H. Matsuo, T. Eto, T. Omae, et al. 1994. Clinical studies on the sites of production and clearance of circulating adrenomedullin in human subjects. *Hypertension* 24:600–604.
 35. Iwasaki, H., S. Eguchi, M. Shichiri, F. Marumo, and Y. Hirata. 1998. Adrenomedullin as a novel growth-promoting factor for cultured vascular smooth muscle cells: role of tyrosine kinase-mediated mitogen-activated protein kinase activation. *Endocrinology* 139:3432–3441.